

KENTUCKY
TRANSPORTATION
CENTER

College of Engineering

**REINFORCEMENT ALTERNATIVES FOR CONCRETE
BRIDGE DECKS**



Research Report
KTC-03-19/SPR-215-00-1F

REINFORCEMENT ALTERNATIVES FOR CONCRETE BRIDGE DECKS

by

Chris Hill
Structural Engineer,
Prestressed Services, Inc.

Choo Ching Chiaw
Research Assistant, Department of Civil Engineering
University of Kentucky

and

Issam E. Harik
Professor of Civil Engineering and Head, Structures Section,
Kentucky Transportation Center

Kentucky Transportation Center
College of Engineering, University of Kentucky

in cooperation with

Transportation Cabinet
Commonwealth of Kentucky

and

Federal Highway Administration
U.S. Department of Transportation

The contents of this report reflect the views of the authors who are responsible for the facts and accuracy of the data presented herein. The contents do not necessarily reflect the official views or policies of the University of Kentucky, the Kentucky Transportation Cabinet, nor the Federal Highway Administration. This report does not constitute a standard, specification or regulation. Manufacturer or trade names are included for identification purposes only and are not to be considered an endorsement.

July 2003

Technical Report Documentation Page

1. Report No. KTC-03-19/SPR-215-00-1F	2. Government Accession No.	3. Recipient's Catalog No.	
4. Title and Subtitle Reinforcement Alternatives for Concrete Bridge Decks (KYSPR 00-215)		5. Report Date July 2003	
		6. Performing Organization Code	
7. Author(s): Chris Hill, Choo Ching Chiaw, and Issam Harik		8. Performing Organization Report No. KTC-03-19/SPR-215-00-1F	
9. Performing Organization Name and Address Kentucky Transportation Center College of Engineering University of Kentucky Lexington, Kentucky 40506-0281		10. Work Unit No. (TRAIS)	
		11. Contract or Grant No. KYSPR 00-215	
		13. Type of Report and Period Covered Final	
12. Sponsoring Agency Name and Address Kentucky Transportation Cabinet State Office Building Frankfort, Kentucky 40622		14. Sponsoring Agency Code	
		15. Supplementary Notes Prepared in cooperation with the Kentucky Transportation Cabinet and the U.S. Department of Transportation, Federal Highway Administration.	
16. Abstract This report investigates the application of various reinforcement types in concrete bridge decks as potential replacements or supplements to conventional steel reinforcement. Traditional epoxy coated reinforcement (ECS), stainless steel clad (SSC) reinforcement, MMFX microcomposite reinforcement, and carbon fiber reinforced polymer (CFRP) reinforcement were evaluated. Tests were conducted to determine the material properties of each reinforcement type. Full-scale two-span reinforced concrete deck specimens were load tested to evaluate their performance. CFRP reinforcement was deployed in a single-span bridge located on Elkin Station Road in Clark County, KY. The SSC and MMFX reinforcements were each placed in a separate span in a two-span bridge located on Galloway Road in Scott County, KY. Results of the laboratory investigation showed that bridge decks reinforced with ECS, SSC, MMFX, and CFRP reinforcements satisfy the AASHTO Specification strength requirements.			
17. Key Words Bridge Deck, Reinforcement, Stainless Steel Clad, MMFX Microcomposite, Carbon Fiber Reinforced Polymer, Epoxy Coated Steel		18. Distribution Statement Unlimited with approval of Kentucky Transportation Cabinet	
19. Security Classif. (of this report) Unclassified	20. Security Classif. (of this page) Unclassified	21. No. of Pages 35	22. Price

TABLE OF CONTENTS

LIST OF TABLES	II
LIST OF FIGURES	III
EXECUTIVE SUMMARY	V
ACKNOWLEDGMENTS	VIII
1.0 INTRODUCTION	1
2.0 MATERIAL PROPERTIES AND BEHAVIORS	2
2.1 Direct Tension Tests of Reinforcements	2
2.2 Concrete Compressive Strengths and Stress-Strain Relations	8
3.0 EXPERIMENTAL SETUP AND PROCEDURES	10
3.1 Introduction	10
3.2 Test Setup	10
4.0 MOMENT-CURVATURE AND EXPERIMENTAL RESULTS	18
4.1 Moment-Curvature Analysis	18
4.2 AASHTO Moments	18
4.3 Experimental Results	20
4.4 Conclusion	22
5.0 CONCLUSIONS AND RECOMMENDATIONS	24
REFERENCES	25

LIST OF TABLES

Table 2.1	Summary of Direct Tensile Test Results of Reinforcing Bars for Concrete Deck Panels	7
Table 2.2	Summary of Concrete Compressive Strengths	8
Table 4.1	Comparison on AASHTO Factored Design Moment and Analytical/Experimental Results	23
Table 4.2	Comparison of AASHTO Factored Design Moment, Analytical Results and Experimental Results with a 20% Redistribution of Moments	23

LIST OF FIGURES

Figure 2.1	Schematic of CFRP Test Specimen	3
Figure 2.2	Direct Tension Tests: (a) Test Specimens; and (b) Test Specimen in Universal Testing Machine (UTM)	3
Figure 2.3	Direct Tension Tests: (a) Tension Fracture of CFRP Bar; (b) Tension Fractures of ECS Bars; (c) Tension Fracture of MMFX Bars; and (d) Tension Fracture of SSC Bars	4
Figure 2.4	Stress-strain Curves for Axial Loaded Epoxy Coated Reinforcement	5
Figure 2.5	Stress-strain Curves for Axial Loaded Strainless Steel Clad Reinforcement	5
Figure 2.6	Stress-Strain Curves for Axial Loaded MMFX Reinforcement	6
Figure 2.7	Stress-Strain Curves for Axial Loaded Carbon Fiber Reinforced Polymer Reinforcement	6
Figure 3.1	Bridge Deck Cross Section showing Regions of Interest	10
Figure 3.2	Typical Slab Panel	13
Figure 3.3	Test Frames showing the Two-Span Slab Panel	14
Figure 3.4	Laboratory Preparation of Two-span Slab Panels	15
Figure 3.5	Single Span Spread Box Beam Bridge in Clark County, KY on Elkin Station Road	16
Figure 3.6	Two-span Bridge in Scott County, KY on Galloway Road	17
Figure 4.1	Analytical Moment-Curvature Plots based on Test Specimen Geometry and Reinforcement	19
Figure 4.2	Analytical Moment-Curvature Plots based on Constant Reinforcement ratio, ρ , and Concrete Strength of 4000 psi	19

Figure 4.3	Crack Patterns at the Initial Cracking Load at the Positive Region (Top-surface) of the MMFX Slab Panel	20
Figure 4.4	Crack Patterns at the Ultimate Load at the Positive Region (Top-surface) of the MMFX Slab Panel	21
Figure 4.5	Profile of the deflected shape of the CFRP slab panel prior to failure	21

EXECUTIVE SUMMARY

The objective of this study is to evaluate the performance of a variety of reinforcement types for concrete bridge decks. Reinforcement types considered in this study consisted of Epoxy Coated Reinforcement (ECS), Stainless Steel Clad Reinforcement (SSC), MMFX Reinforcement, and Carbon Fiber Reinforced Polymer Reinforcement (CFRP). The objective was achieved by conducting the following tasks: (1) Direct tensile tests on samples of each reinforcement type; (2) Laboratory testing of two-span concrete slab panels reinforced with each type of reinforcement; (3) Comparison of laboratory test results with analytical analyses and AASHTO Specification requirements; (4) Deployment of SSC and MMFX reinforcement in the Galloway Road bridge deck in Scott County, KY and CFRP reinforcement in the Elkin Station Road bridge deck in Clark County, KY.

MATERIAL PROPERTIES AND BEHAVIOR

ASTM A 370 (AASHTO T 244) tensile test procedures were applied in the testing of the steel reinforcement specimens. Tensile tests of the CFRP reinforcement were conducted in accordance with the “ACI Standard Test Method for Tensile Strength and Modulus of FRP Rod”. Stress-strain behavior of each reinforcement type was established by means of disposable strain gages and dial gage measurements over a predefined gage length.

For both the ECS and SSC reinforcement a well-defined elastic-plastic, stress-strain response was obtained. Representative values for the Elastic Modulus and Yield Stress were obtained for use in the analytical analysis of the ECS and SSC panels. The MMFX reinforcement presents an initially linear stress-strain response followed by an extensive non-linear response to failure. In the absence of a well-defined yield plateau the MMFX reinforcement was modeled with the expression of Richard and Blalock (1969) for the analytical analysis of the MMFX panel. CFRP reinforcement remains linear-elastic to failure and was therefore modeled analytically on the basis of an average Elastic Modulus.

LABORATORY TESTING OF TWO-SPAN SLAB PANELS

One full-scale concrete slab panel for each type of reinforcement was tested to simulate transverse bridge deck load conditions. Each specimen was reinforced with a top and bottom mat of the respective reinforcement types with transverse bars of the same type spaced in accordance with the AASHTO Specifications for bridge slabs. Each panel was supported as a two-span continuous slab with six (6) feet spans. Six (6) feet spans were selected as being representative of the design span of typical bridge decks. Furthermore, wheel loads for the AASHTO design truck are spaced transversely at six (6) feet such that simultaneous application of loads at mid-span of each span would accurately reflect the loading configuration anticipated by the AASHTO Specifications.

All of the slab panels exhibited extensive cracking prior to failure. In each case failure was associated with diagonal shear, however, substantial ductility was exhibited through relatively large displacements, large crack widths and extensive cracking prior to collapse.

COMPARISON WITH AASHTO SPECIFICATIONS

Comparisons of the slab panel results to current AASHTO Standard Specification provisions for bridge deck design show that all of the deck panels exceeded AASHTO guidelines for ultimate load. Although each of the specimens failed in diagonal shear, the AASHTO specifications are based on under-reinforced sections with steel reinforcement, failing after yielding of the reinforcing steel. Based on measured load limits, the size of cracks and the extensive cracking in both positive and negative moment regions all of the steel reinforced specimens behaved as under-reinforced sections. The CFRP panel behaved as an over-reinforced section as intended by the recommendations of ACI 440K. The panel resisted a load far in excess of that required by the Standard Specifications while exhibiting, large cracks and localized crushing of concrete at the interior support. Consequently, while the final failure mode of all specimens was in diagonal shear, it is apparent that all specimens were sufficiently ductile and provided ample warning of impending collapse before final failure occurred.

DEPLOYMENT OF REINFORCEMENT IN BRIDGE DECKS

Each of the reinforcement types investigated in this study has been successfully deployed in in-service bridge decks. ECS reinforcement, being the traditional reinforcement utilized for many years, is the standard by which other reinforcements are evaluated.

The SSC and MMFX reinforcement were placed in a two-span bridge in Scott County, KY on Galloway Road. All longitudinal reinforcement in the bridge was epoxy coated while all top and bottom transverse reinforcement in span 1 was MMFX reinforcement and all top and bottom transverse reinforcement within span 2 was SSC reinforcement. [Note: The Kentucky Transportation Cabinet (KyTC) elected to utilize uncoated, black steel with cathodic protection as top and bottom transverse reinforcement in a small portion of span 2].

CFRP reinforcement was placed in a single-span spread box beam bridge in Clark County, KY on Elkin Station Road. All longitudinal and transverse reinforcement in both the top and bottom mats are CFRP bars.

CONCLUSIONS

Results of this study demonstrate that AASHTO Standard Specification provisions for the strength design of bridge decks are satisfied by all of the reinforcement types (CFRP, MMFX, Stainless Steel Clad, and Epoxy Coated Steel Reinforcements) evaluated in this study. Considerable load redistribution and extensive cracking prior to failure indicates that each of the reinforcement types experienced sufficient straining to insure ductile failure of bridge decks reinforced with any of the tested materials. Similar numbers of cracks, similar crack patterns, and crack sizes, demonstrate that any of the reinforcement types can be expected to behave satisfactorily for span lengths up to six (6) feet. In-service performance of the various reinforcements in actual bridges has further demonstrated their adequacy.

ACKNOWLEDGMENTS

Financial support for this project was provided by the Federal Highway Administration, the Kentucky Transportation Cabinet, and the National Science Foundation under grant CMS-9601674-ARI program.

The authors would like to acknowledge the laboratory assistance of undergraduate students: Louis Mattingly, Roy Sturgill, Robert Goodpaster.

1.0 INTRODUCTION

Historically, transportation departments have been burdened with substantial maintenance costs associated with the repair or replacement of bridge decks resulting from corrosion induced deterioration. Corrosion deterioration of reinforced concrete bridge decks is brought about by the application of deicing salts to the bridge deck to melt ice and snow during winter months. Bridge decks are highly susceptible to chloride ion damage to the steel used to reinforce the concrete because the deicing salts are placed directly on the riding surface.

The most common solution to the corrosion deterioration problem is the use of coated steel reinforcements such as epoxy coated steel (ECS). Scattered through the literature are reports of success and failure in the utilization of ECS. Due to the multitude of factors that influence the overall performance of bridge decks it can only be concluded that ECS is not a guaranteed method of preserving reinforced concrete bridge decks. Consequently, efforts continue to identify alternative reinforcements that may prolong the service life of bridge decks.

Three potential alternatives are Stainless Steel Clad black steel (SSC), MMFX Microcomposite reinforcement (MMFX) and Carbon Fiber Reinforced Polymer (CFRP) reinforcement. The non-corrosive nature of stainless steel provides the potential for simply using the stainless steel as a protective cladding to the interior black steel in a manner similar to the use of epoxy coating or galvanizing. MMFX reinforcement is metallurgically altered to eliminate grain boundaries at which corrosion initiates. MMFX steel is reported to provide an extended time to initial corrosion and a substantially slower corrosion rate, both of which suggest an extended service life may be achieved by the MMFX reinforced bridge deck. Lastly, CFRP is not only inherently corrosion resistant but also provides high strength and stiffness to weight ratios.

2.0 MATERIAL PROPERTIES AND BEHAVIOR

2.1 Direct Tension Tests of Reinforcements

Direct tension tests were conducted on Epoxy Coated Steel (ECS), Stainless Steel Clad (SSC), MMFX Microcomposite Steel, and Carbon Fiber Reinforced Polymer (CFRP) reinforcing bars to determine specific tensile properties. These tensile properties include the yield strength (σ_y), ultimate strength (σ_u), elastic modulus (E), and rupture strain (ϵ_r), where applicable.

Tension tests on the various steel bars were conducted in accordance with the ASTM A370-92 specification. The preparation process of the steel test specimens can be summarized in the following steps:

1. Test specimens with a length of approximately 30 in. (750 mm) were prepared.
2. An area of the bar at its midpoint, just large enough to accept a ¼" disposable strain gage, was ground to a smooth finish.
3. A strain gage was glued to the bar and wired to an automated data acquisition system.
4. The specimens were then placed in the grips of a hydraulic testing machine and loaded to failure. Multiple loading cycles were employed in several instances to assure stability of the resulting measurements.
5. For comparative purposes, some of the bars were fitted with a dial gauge pinned between two fixed points on either side of the strain gage. Dial gauge measurements of the tensile deformation were measured over an eight (8) inch gauge length.

The preparation process of the CFRP test specimens can be summarized in the following steps with the aid of Fig. 2.1.

1. Test specimens with a length of approximately 60 in. (1500 mm) were prepared.
2. To grip the test specimens, a steel pipe with a length of 10 in. (250 mm) was cut lengthwise into two pieces.
3. Small pin holes were drilled in the individual halves of the steel pipe to allow air to reach the two-part epoxy utilized as described in following step.
4. After cleaning the inner surface of the pipe and the ends of the test specimens, a two-part metal epoxy was applied to the interior surfaces of the semi-circular steel pipes. They were clamped at the ends of the test specimens until the epoxy was completely cured (curing took approximately seven days).
5. Once the epoxy cured, strain gages were glued to the specimens as described earlier for the steel bars and the specimens were tested in a similar manner.

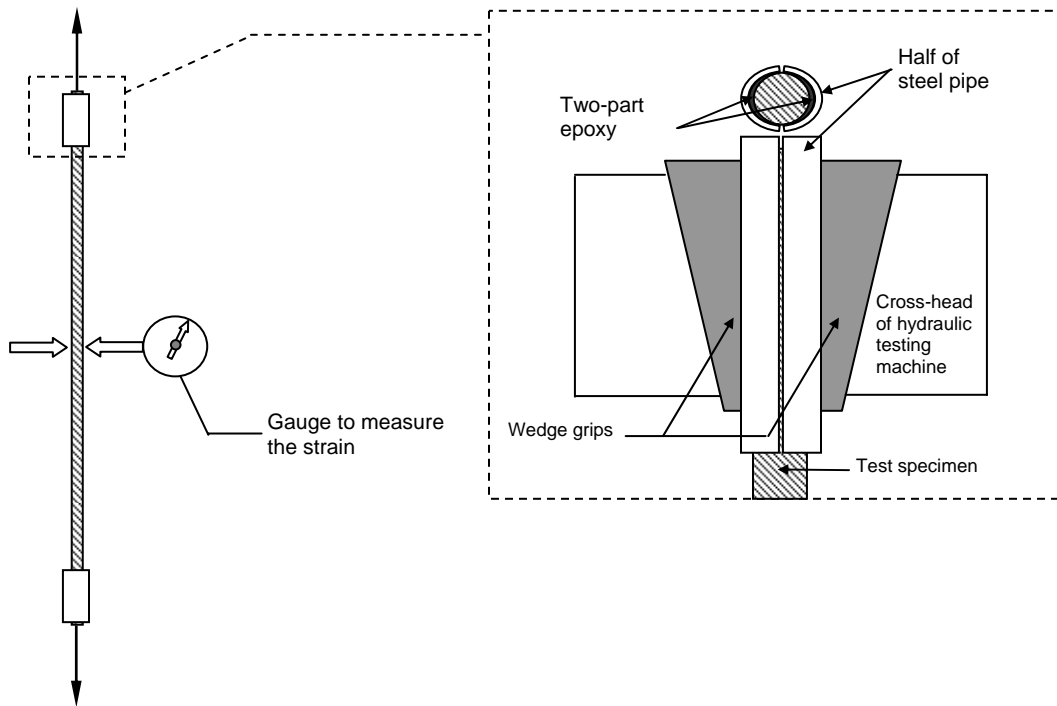
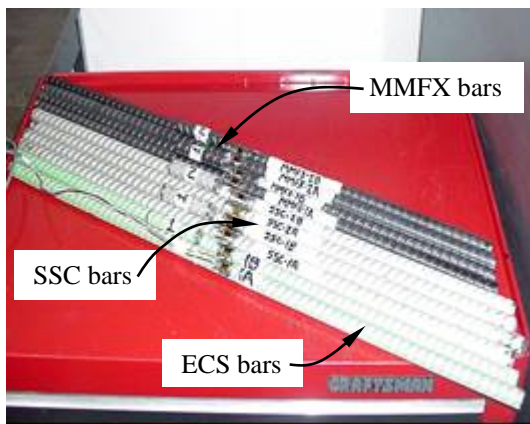
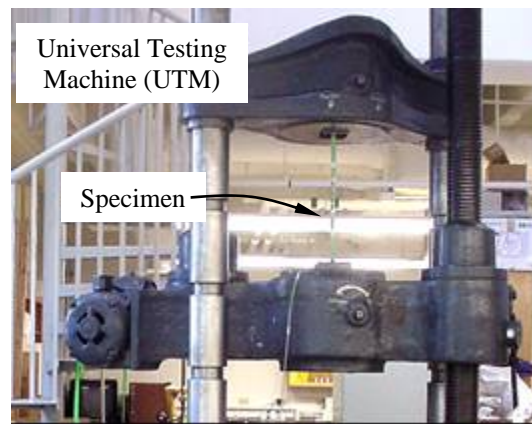


Figure 2.1. Schematic of CFRP test specimen.



(a)



(b)

Figure 2.2. Direct tension tests: (a) Test specimens; and (b) Test specimen in Universal Testing Machine (UTM).

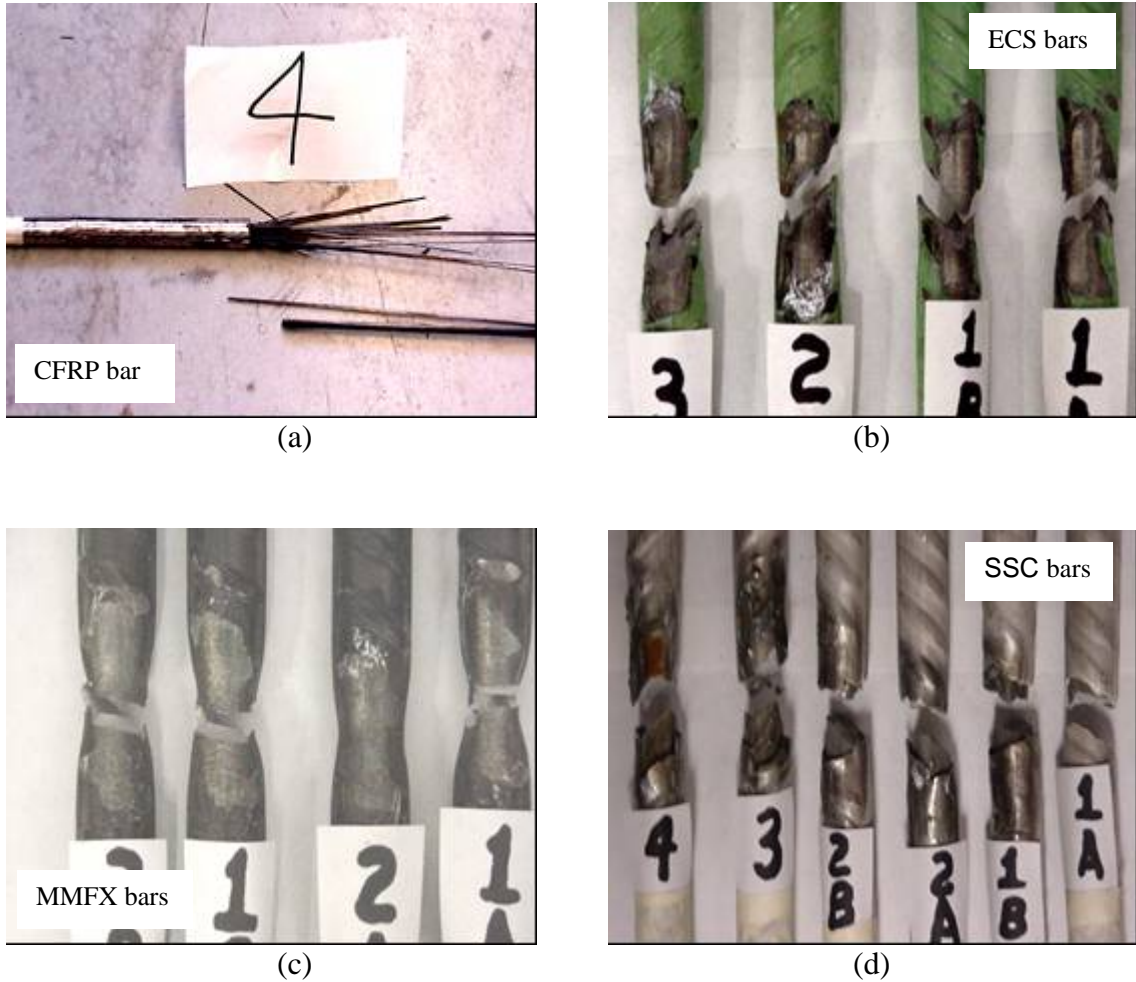


Figure 2.3. Direct tension tests: (a) Tension fracture of CFRP bar; (b) Tension fracture of ECS bars; (c) Tension fracture of MMFX bars; and (d) Tension fracture of SSC bars.

Fig. 2.2 shows the different bar types prepared for the direct tension tests. The tests were performed using the Universal Testing Machine (UTM) shown in Fig. 2.2(b). Tension fractures of different bar types are depicted in Fig. 2.3:

Stress-strain plots for each of the specimens are shown in Figures 2.4 to 2.7. Yield stress values for the ECS and SSC reinforcement were taken from the shape of the stress-strain diagrams shown in Figures 2.4 and 2.5. Ultimate stress values for each reinforcement type were computed based on the load at rupture and an approximate cross-sectional area at the location of the attached strain gage. In all tensile tests rupture occurred at the location of the strain gage.

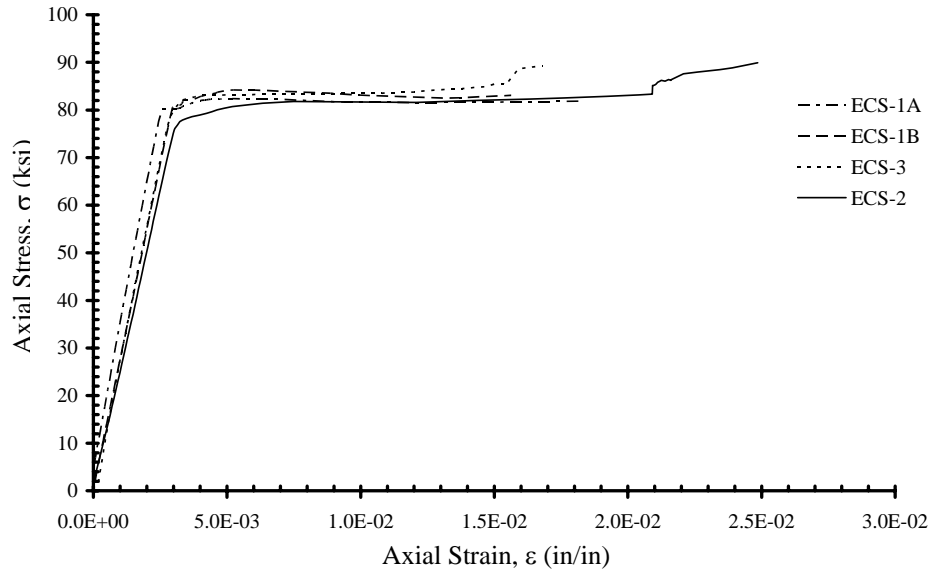


Figure 2.4. Stress versus Strain for axial loaded Epoxy Coated Reinforcement

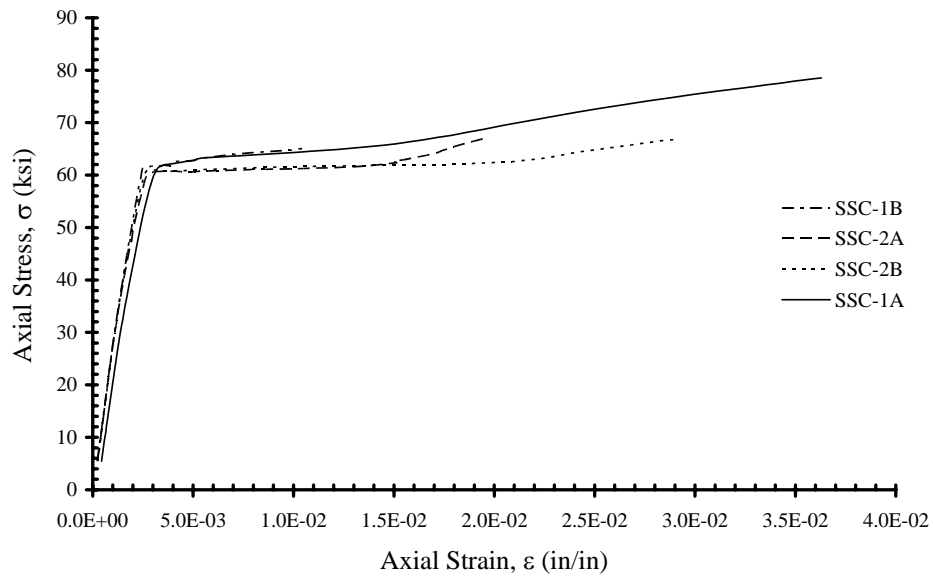


Figure 2.5. Stress versus Strain for axial loaded Stainless Steel Clad Reinforcement

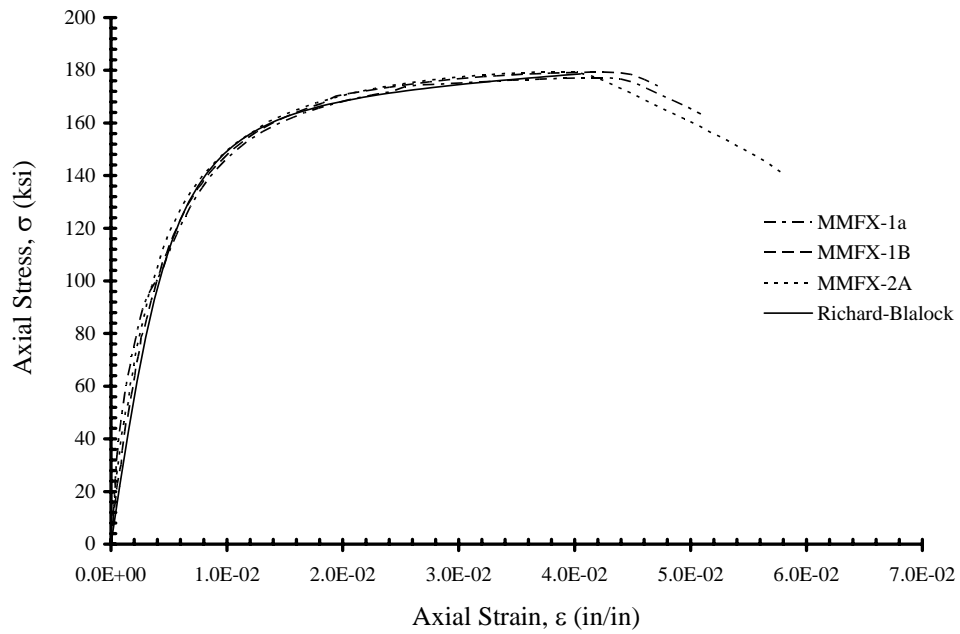


Figure 2.6 Stress versus Strain for axially loaded MMFX Reinforcement

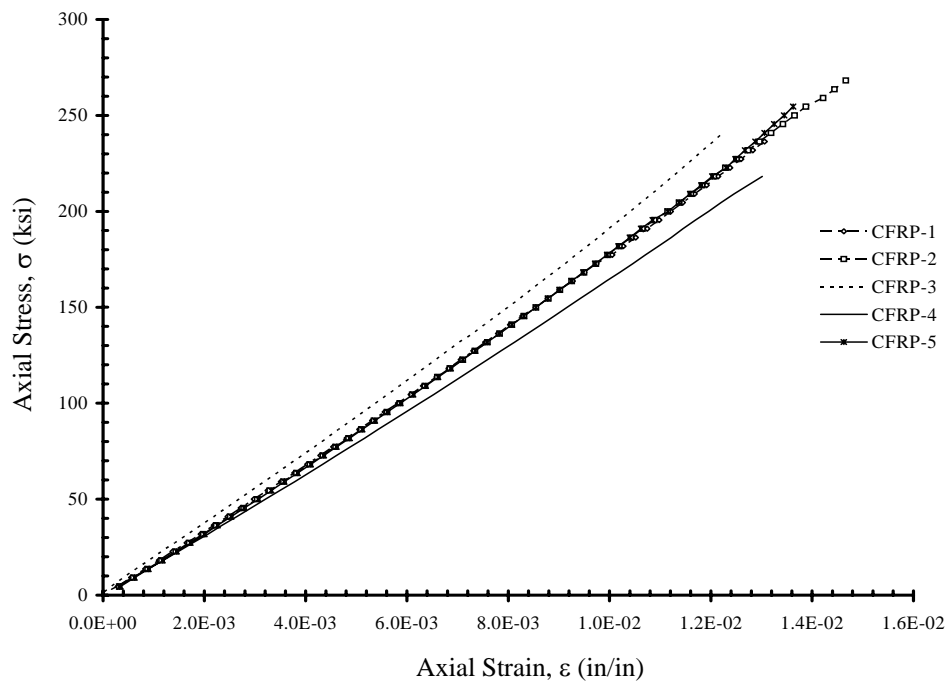


Figure 2.7. Stress versus Strain for axially loaded Carbon Fiber Reinforced Polymer Reinforcement

Elastic modulus values are based on linear regression of the stress-strain data acquired from the strain gages. The respective regressions were carried over a stress region in which the stress-strain relationship was essentially linear. Specifically, the regression analysis of the ECS reinforcement was performed from zero (0) to fifty (50) ksi. The regression analysis of the SSC reinforcement was performed from zero (0) to thirty (30) ksi and the regression analysis for the MMFX reinforcement was performed from zero (0) to thirty-six (36) ksi. A regression analysis was performed on each loading cycle applied to the particular specimen. Since the CFRP reinforcement is linear to rupture, in accordance with ACI 440K Guide Test Methods for Fiber Reinforced Polymer (FRP) Rods and Sheets, the regression analysis was performed over a range of 20% to 60% of the tensile capacity of the specimen. The resultant elastic moduli reported in Table 2.1 are the average of all values for each type of reinforcement.

Rupture strains are also average values for each reinforcement type, except as noted below, based on an original gauge length of eight (8) inches divided by the pieced-together length of the failed specimen (as provided for in ASTM A 370-92).

Table 2.1 Summary of direct tensile test results of reinforcing bars for concrete deck panels.

Bar Type	# of specimen tested	σ_y , ksi (Mpa)	σ_u , ksi (MPa)	E , ksi (GPa)	ϵ_r , (%)
(1)	(2)	(3)	(4)	(5)	(6)
ECS ⁽¹⁾	4	81 (560)	105 (725)	29000 (200)	11.2
SSC ⁽¹⁾	6	61 (420)	90 (620)	27000 (185)	12.1
MMFX ⁽²⁾	4	N/A	180 (1240)	29500 (205)	12.1
CFRP ⁽³⁾	5	N/A	270 (1875)	18300 (125)	*1.33

Notes:

- ⁽¹⁾ Steel reinforcing bars that have a well defined yield stress
- ⁽²⁾ Metallurgically altered micro-composite steel without a well defined yield stress
- ⁽³⁾ Carbon fiber-reinforced polymer (CFRP) reinforcing bars are linear-elastic until failure
- * Elongation at failure of strain gage, actual elongation at rupture was greater but unknown

Stress-strain relationships for the ECS and SSC reinforcement required for the theoretical moment-curvature analyses are assumed to be linearly-elastic, perfectly-plastic. Strain hardening has been ignored since strains are generally within the yield plateau and design code, moment capacity computations neglect strain hardening. CFRP reinforcement, however, is linearly-elastic to rupture.

Experimental stress-strain curves of MMFX reinforcement are initially linear but then highly nonlinear at higher stress levels. In this study, the stress-strain behavior of the MMFX reinforcement is modeled using the Richard and Blalock (1969) expression:

$$\sigma(\varepsilon) = \frac{E\varepsilon}{\left\{ 1 + \left[\frac{E\varepsilon}{\left(1 - \frac{E_t}{E}\right)\sigma_k + E_t\varepsilon} \right]^n \right\}^{\frac{1}{n}}} \quad (2.1)$$

where,

- E = Initial Elastic Modulus
- E_t = Post-Yield Elastic Modulus
- σ_k = Characteristic Yield Stress
- n = Characteristic exponential
- ε = Strain

2.2 CONCRETE COMPRESSIVE STRENGTHS AND STRESS-STRAIN RELATIONS

The compressive strength, f'_c , for the concrete deck panels were determined in accordance with ASTM Standard C39. Three 6 in. x 12 in. cylinders for each type of deck panel were prepared and cured under standard laboratory conditions, and tested at a specified rate of loading on the date of the respective slab panel test to obtain individual cylinder compressive strengths. The results of compressive strength tests are presented in Table 2.2.

Table 2.2 Summary of concrete compressive strengths.

Type of Deck Panel	Compressive strengths, f'_c psi (Mpa)			Average Compressive Strengths, f'_c psi (MPa)
	Cylinder #1	Cylinder #2	Cylinder #3	
(1)	(2)	(3)	(4)	(5)
ECS	4,524 (31.2)	4,265 (29.4)	4,817 (33.2)	4,535 (31.3)
SSC	4,216 (29.1)	4,202 (29.0)	3,664 (25.3)	4,027 (27.8)
MMFX	4,343 (29.9)	4,184 (28.8)	4,329 (29.8)	4,285 (29.5)
CFRP	4,025 (27.8)	4,251 (29.3)	3,523 (24.3)	3,933 (27.1)

Analytical modeling of the individual slab panel concrete was based on their respective average compressive strengths and the Hognestad (1951) concrete stress-strain relationship expressed as follows:

$$f_c = \phi f_c' \left\{ \frac{2\varepsilon_c}{\varepsilon_o} - \left(\frac{\varepsilon_c}{\varepsilon_o} \right)^2 \right\} \quad (2.2)$$

$$f_c = \phi f_c' \left\{ \varepsilon_o - 0.15 \frac{(\varepsilon_c - \varepsilon_o)}{(\varepsilon_{cu} - \varepsilon_o)} \right\} \quad (2.3)$$

where,

f_c = concrete stress, psi.

f_c' = specified concrete compressive strength, psi

ε_c = concrete strain, in/in.

ε_{cu} = maximum usable concrete strain, in/in.

$\varepsilon_o = \frac{\phi(2f_c')}{E_c}$ = concrete strain at specified concrete compressive strength, in/in.

$E_c = 33w_c^{1.5} \sqrt{f_c'}$ (ACI 318-02) = secant modulus of elasticity of concrete.

ϕ = modifier accounting for casting orientation (0.85 for vertical, 0.9 for horizontal, taken as one (1) in this study)

3.0 EXPERIMENTAL SETUP AND PROCEDURES

3.1 Introduction

Figure 3.1 shows a cross section of a typical bridge deck designed to transfer vehicle loads from the riding surface to the main support girders of a bridge superstructure. Typically, bridge decks are designed to transfer loads to main support girders in a direction transverse to traffic flow. Four slab panels were tested to evaluate the behavior of bridge decks in the transverse direction reinforced with different types of reinforcement including epoxy coated steel (ECS), stainless steel clad (SSC), MMFX Microcomposite steel (MMFX) and carbon fiber reinforced polymer (CFRP) bars.

The deck panels were constructed and tested to simulate the two regions of a bridge deck highlighted in Figure 3.1.

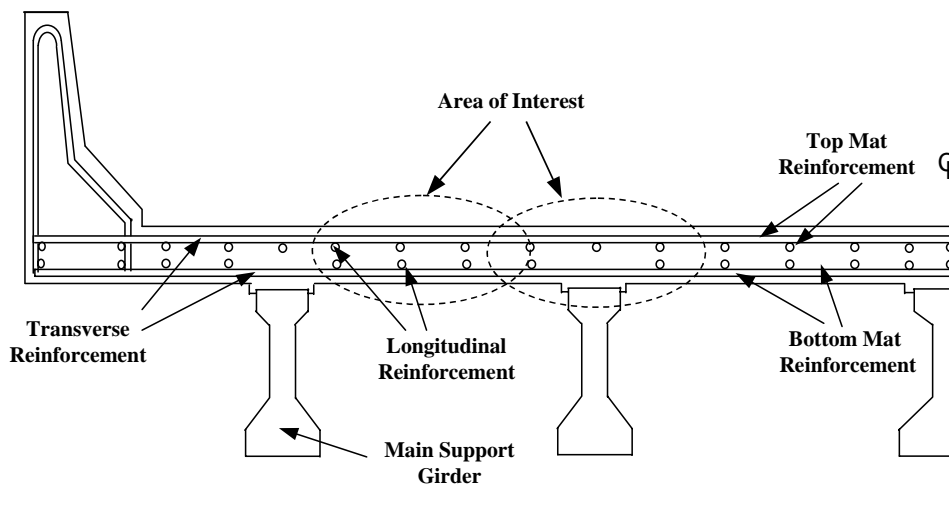


Figure 3.1. Bridge Deck Cross Section Showing Regions of Interest

3.2 Test Setup

Each slab panel was constructed to nominal dimensions of 7 ½" x 33" x 13'-6". The dimensions were selected to represent the traditional design thickness, 7 ½", used by the KyTC, to accommodate some degree of longitudinal load distribution from the tire contact area discussed later, and to provide two six (6) feet spans simulating a typical bridge with a six (6) feet girder spacing. A plan and profile of the slab panel specimens is shown in Figure 3.2. Included in the figure are the support conditions, applied loads and data acquisition elements.

Free rotation was accommodated at each support location by use of steel half-rounds. Localized crushing, or spalling, of concrete was prevented by placing a load

distribution plate under the half-round and on top of an elastomeric bearing pad that rested on the slab panel. Vertical movement was prevented at each support location by anchoring the test frame to the laboratory floor (see Figure 3.3).

Hydraulic jacks were used to apply loads to the deck panels at a six (6) feet spacing simulating the wheel loads of an AASHTO Specification Design Truck. Since the slab panels were supported at a six (6) feet spacing and the loads were also applied at a six (6) feet spacing, this single load configuration closely approximated a worst case loading for both the positive and negative moment regions highlighted in Figure 3.1.

The individual applied loads were distributed over an area approximating the AASHTO tire contact area. By the Specifications, the tire contact area is defined as being 20" x 10" such that an HS20 loading (a 20 kip wheel load) produces a contact pressure of 100 psi. Utilizing available laboratory materials the experimental test setup provided a contact area that was 22" x 9". Parallel hydraulic lines emanating from a single hydraulic pump insured equal pressures, and therefore equal loads, were applied at each jack location.

The respective concrete covers used in the slab panels were selected for the following reasons. First, a 2" cover to the top mat of the ECS specimen is consistent with the current practice of the KyTC in the construction and analysis of their bridge decks. That is to say, top mat ECS bars are located at 2 ½" during construction but the structural analysis of the deck is based on the assumption that ½" of the cover concrete will be worn away or otherwise become ineffective in resisting load. Similarly, the bottom mat reinforcement of all panels was placed at a 1" cover to be consistent with the current practice of the KyTC.

A 1" cover to the top mat of the SSC, MMFX and CFRP panels was selected in consideration of the enhanced corrosion resistance promised by each of these three types of reinforcement. Assuming these bars are immune to corrosion they could be placed at a construction cover of 1 ½" and the structural analysis of the deck would again assume that ½" of the cover concrete is sacrificial concrete. The increased efficiency of a reduced cover, measured by comparison of appropriate moment-curvature analyses and experimental failure loads, might then be demonstrated within this study.

As depicted in Figure 3.2, disposable foil strain gages were glued to three (3) of the five (5) bars in each mat of reinforcement at the locations of interest. That is to say, at midspan of each span for positive moments and at the interior support for negative moments. A single Linear Variable Displacement Transducer (LVDT) was placed at the centerline of the specimen under each support location to monitor support movement. Two (2) LVDT's were located at midspan of each span to measure deflections resulting from flexure of the slab panel.

Laboratory preparation of slab panels is shown in Figure 3.4. The completed bridge structures in Clark County and Scotty County are shown in Figures 3.5 and 3.6, respectively. In this study, comparisons of the test results to analytical predictions and code specifications will be included and the results are provided in Chapter 4.

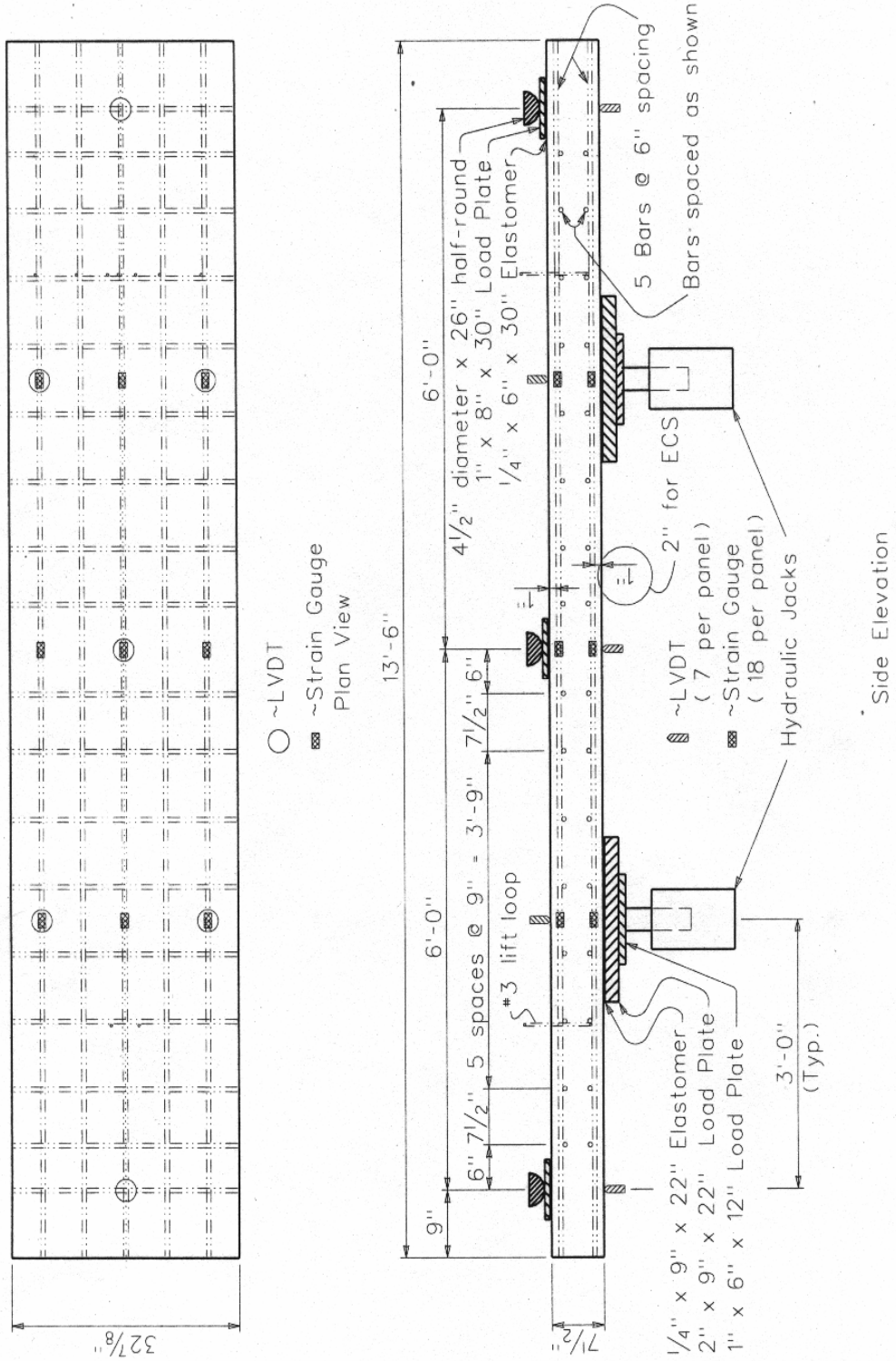


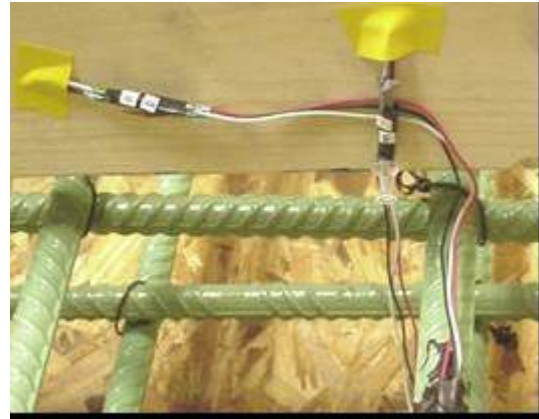
Figure 3.2. Typical Slab Panel



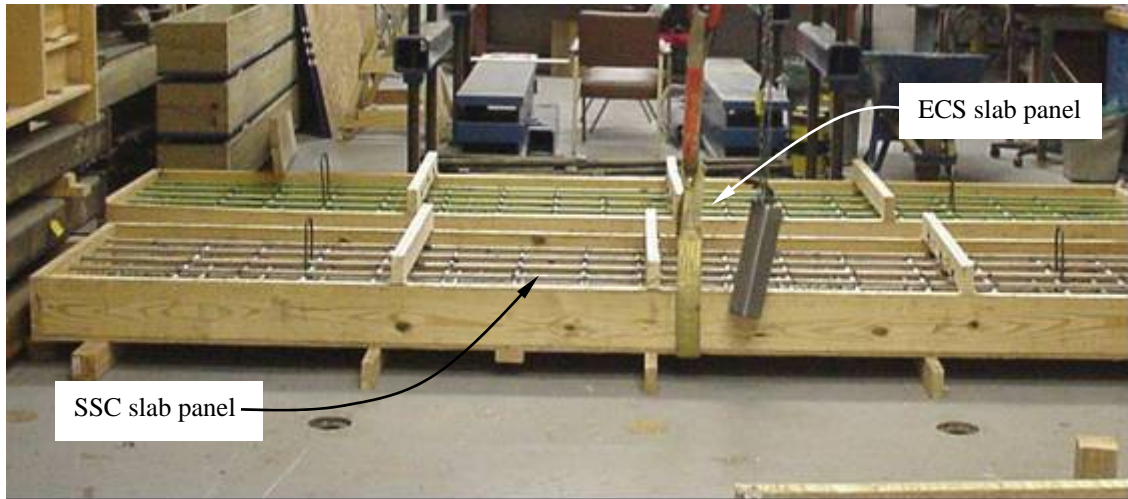
Figure 3.3. Test frames showing the two-span slab panel.



(a)



(b)

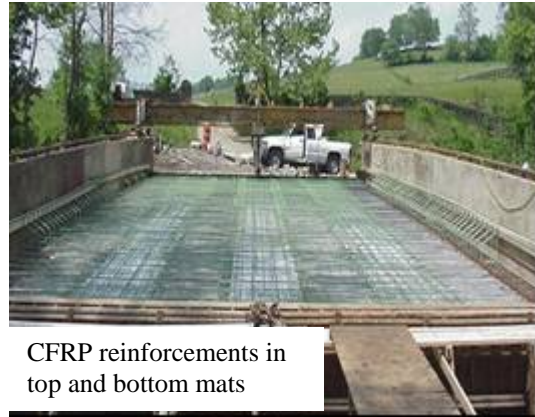


(c)

Figure 3.4. Laboratory preparation of two-span slab panels: (a) Form-work for 7-1/2" x 33" x 13'-6" two-span slab panels; (b) placement and wiring of strain gauges onto slab reinforcement; (c) completed form-works ready for concrete placement.



(a)



(b)



(c)



(d)



(e)



(f)

Figure 3.5. Single-span spread box beam bridge in Clark County, KY on Elkin Station Road: (a) Construction of single-span bridge; (b) and (c) CFRP reinforcements as longitudinal and transverse reinforcement in both the top and bottom mats; (d) concrete placement; (e) cleaning of bridge deck; and (f) view of completed single-span bridge.



(a)



(b)



(c)

Figure 3.6. Two-span bridge in Scott County, KY on Galloway Road: (a) Construction of two-span bridge; (b) MMFX rebars in Span 1 and SSC rebars in Span 2; and (c) completed structure.

4.0 MOMENT-CURVATURE AND EXPERIMENTAL RESULTS

4.1 Moment-Curvature Analyses

Moment-curvature plots shown in Figure 4.1 for the individual slab panels were based on the average compressive strength for the respective panels presented previously in Table 2.2 of Section 2.2. Each moment-curvature plot is based on a maximum usable concrete compressive strain of 0.003 in/in. Although higher concrete compressive strains were anticipated in the test specimens based on prior experimental work, the AASHTO Specification limit of 0.003 in/in. was adopted to facilitate a more direct comparison of the performance of the various slab panels with the Specifications.

For purposes of evaluating the relative performance of each reinforcement type when substituted on a one-for-one basis, the experimental slab panels were reinforced with the same number of bars (5 bars) which effectively results in a different reinforcement ratio, ρ , for each panel. The different ratios are shown in Fig. 4.1.

To simulate the anticipated performance of each reinforcement type when the same reinforcement ratio was employed for each slab panel, moment-curvature analyses were performed. The results of the moment-curvature analyses are generated and shown in Fig. 4.2. In this case, the reinforcement ratio of 0.00757 was selected, and this is in fact the reinforcement ratio of the ECS slab panel in the positive moment section. Each plot in Figure 4.2 is generated based on a concrete strength of 4000 psi.

4.2 AASHTO Moments

For comparison purposes, the AASHTO Specification Service Design Moment and Factored Design Moment are also included in the moment-curvature plot. AASHTO Service Moment was computed by elastic analysis of the two-span panel shown in Fig. 3.2 under the AASHTO HS20 loading (20 kip wheel load). The single wheel load is placed at mid-span of the slab panel to approximate a worst case loading for both the positive and negative moments. The AASHTO Service Moment is 18.8 k-ft as shown in Figs. 4.1 and 4.2. The AASHTO Factored Design Moment is determined using the following equation (AASHTO 2002):

$$M_u = \gamma[\beta_D M_D + \beta_L(M_L)]$$

M_D and M_L are the moments due to dead (self-weight) and live (wheel) loads, respectively. β_D and β_L are the load combination coefficients due to dead and live loads, and are taken as 1.0 and 1.67, respectively. γ is the load factor and is equal to 1.3.

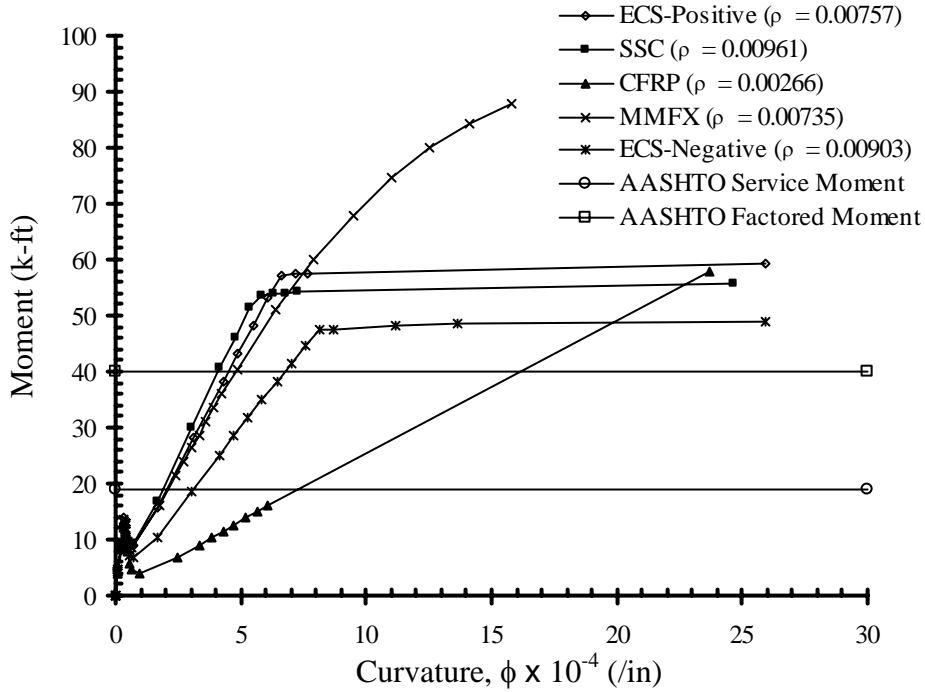


Figure 4.1. Analytical Moment-Curvature Plots based on Test Specimen Geometry and Reinforcement

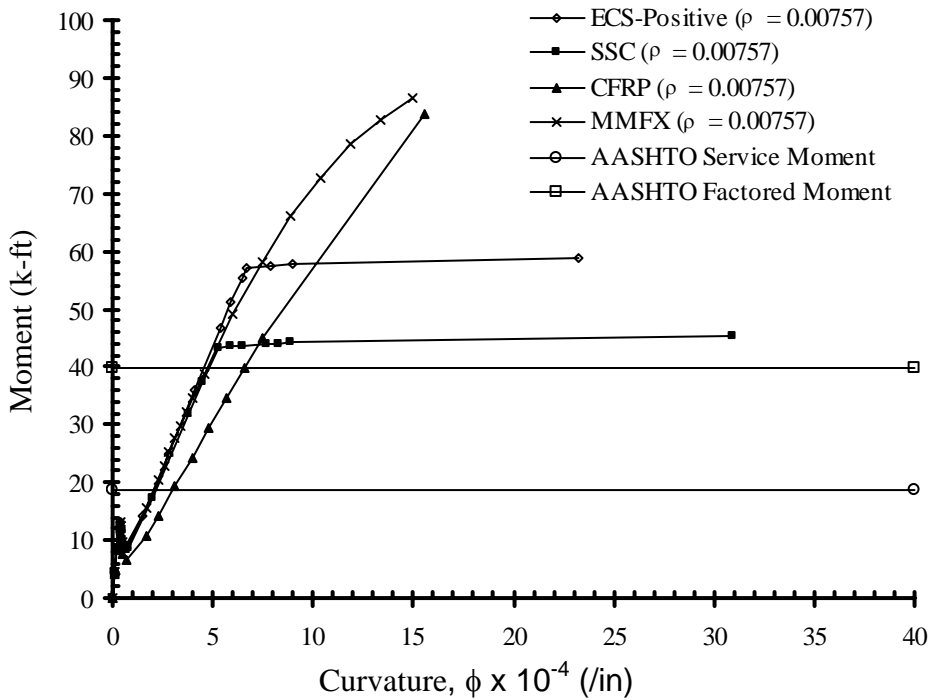


Figure 4.2 Analytical Moment-Curvature Plots based on constant Reinforcement ratio, ρ , and Concrete Strength of 4000 psi.

4.3 EXPERIMENTAL RESULTS

For purposes of comparison the experimentally determined moments at failure, the moment capacities predicted by moment-curvature and the AASHTO Factored Load Design Moment are shown in Table 4.1. Failure moments were computed by elastic analysis of the two-span panel under the experimentally measured load at each jack location. Loads applied in the elastic analysis were treated as line loads distributed over a loaded length of 22", consistent with the dimensions of the load plate depicted in Figure 3.2.

As anticipated the computed elastic moments at the interior support are well in excess of the predicted capacity based on moment-curvature analyses. Furthermore, the mid-span elastic moments are generally below the moment-curvature predictions. A thorough examination of the post-cracking redistribution of load is required to obtain accurate values for the moments present at the failure load. Suffice it to say that actual mid-span moments would increase in association with a reduction in moment at the interior support as cracking occurs at the interior support. This type of redistribution is provided for in Code provisions whereby interior support moments can be decreased by as much as 20% provided mid-span design moments are increased by 20%.

Figures 4.3 and 4.4 depict the development of the top-surface (i.e. positive moment) crack pattern within a single 6-foot span of the MMFX slab panel, the cracking pattern was consistent for each span of all slab panels, as applied load increased from initial cracking to near ultimate load. Not shown is the concurrent cracking occurring on the bottom surface at the interior support (i.e. the negative moment cracking). The ductility of the CFRP slab panel prior to failure is reflected in Figure 4.5.

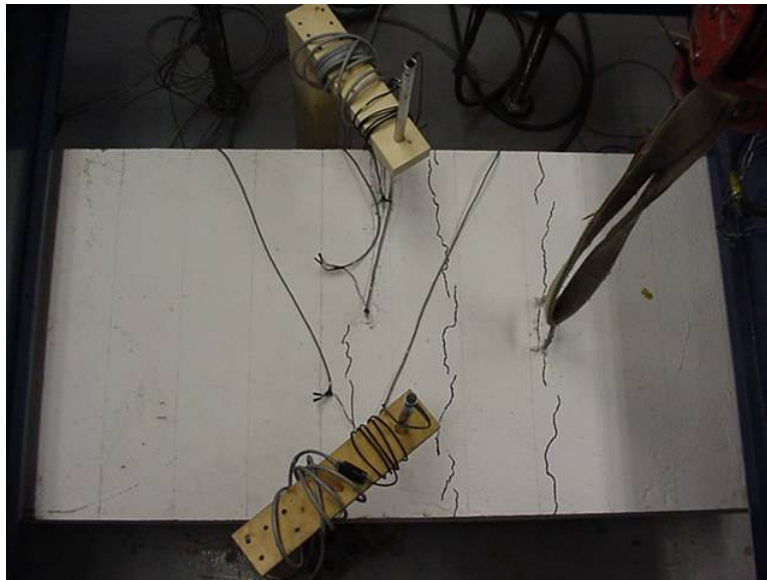


Figure 4.3. Crack patterns at the initial cracking load at the positive moment region (top-surface) of the MMFX slab panel.

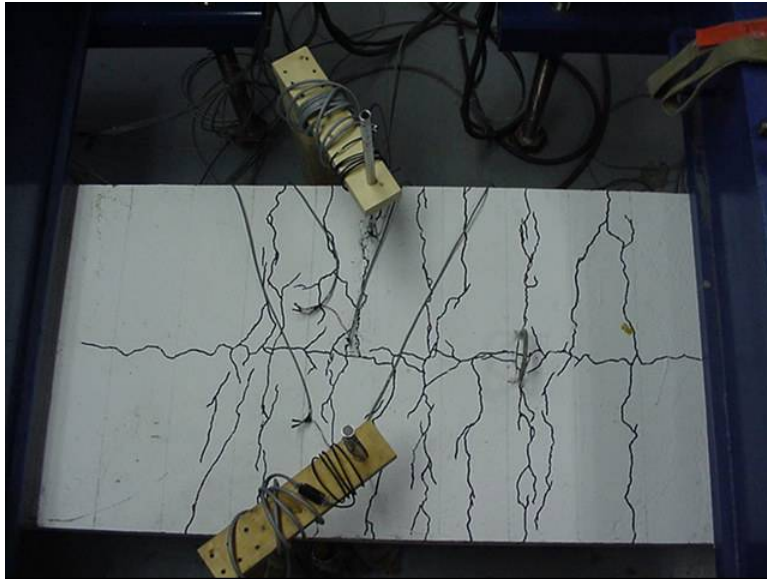


Figure 4.4. Crack patterns at the ultimate load at the positive moment region (top-surface) of the MMFX slab panel.



Figure 4.5. Profile of the deflected shape of the CFRP slab panel prior to failure.

It was intended that strain readings from the various gages attached to the reinforcing bars would provide a means of evaluating the redistribution of moments after the initiation of cracking. Unfortunately, the cracking itself induced localized strain effects in the reinforcement and the strain gage readings could not be relied upon for evaluating moments at either mid-span or at the interior support.

As an alternative to relying on strain gage measurements to establish experimental moments at the cross sections of interest, an assumed redistribution of 20% would produce derived moments as shown in Table 4.2.

4.4 CONCLUSION

Moment capacities of the slab panels were determined analytically and experimentally. In both cases, the moment capacities of each slab panel well exceeded the AASHTO factored design moment. With 20% redistribution of moments permitted by AASHTO Code, the experimental moment capacities consistently exceed the moment capacities predicted by the moment-curvature analyses. This indicates that in each case the mobilization of strains in tensile reinforcement was adequately developed, and that the full bending capacity of the concrete section developed prior to any diagonal shear failure.

Table 4.1 Comparison of AASHTO Factored Design Moment and Analytical/Experimental Results

Bar Type	AASHTO Standard Specification Factored Moment (k-ft)	Moment Curvature Analysis		Moments derived from Experimental Data	
		Positive Moment Capacity (k-ft)	Negative Moment Capacity (k-ft)	Positive Moment Capacity (k-ft)	Negative Moment Capacity (k-ft)
(1)	(2)	(3)	(4)	(5)	(6)
ECS	39.9	59.3	48.9	55.5	81.0
SSC	39.9	55.6	55.6	80.7	117.5
MMFX	39.9	87.9	87.9	75.2	109.4
CFRP	39.9	58.0	58.0	52.6	76.5

Table 4.2 Comparison of AASHTO Factored Design Moment, Analytical Results and Experimental Results with a 20% Redistribution of Moments

Bar Type	AASHTO Standard Specification Factored Moment (k-ft)	Moment Curvature Analysis		Based on Moments derived from Experimental Data	
		Positive Moment Capacity (k-ft)	Negative Moment Capacity (k-ft)	Positive Moment Capacity (k-ft)	Negative Moment Capacity (k-ft)
(1)	(2)	(3)	(4)	(5)	(6)
ECS	39.9	59.3	48.9	66.6	64.8
SSC	39.9	55.6	55.6	96.8	94.0
MMFX	39.9	87.9	87.9	90.2	87.5
CFRP	39.9	58.0	58.0	63.1	61.2

5.0 CONCLUSIONS AND RECOMMENDATIONS

The objective of this study was to evaluate the performance of a variety of reinforcement types for concrete bridge decks. Reinforcement types considered in this study consisted of Epoxy Coated Reinforcement (ECS), Stainless Steel Clad Reinforcement (SSC), MMFX Reinforcement, and Carbon Fiber Reinforced Polymer Reinforcement (CFRP). Direct tension tests were performed to determine tensile properties of the reinforcing bars. In addition, two-span concrete slab panels reinforced with each reinforcement type were cast and tested. The experimental results were then compared with analytical results and AASHTO Specification requirements.

Due to the extensive cracking experienced by each of the slab panels and the practical limitations of accurately measuring crack widths, no definitive conclusions can be provided with respect to the service load performance of the slab panels. Suffice it to say that the ECS panel, used as a point of reference, experienced a similar degree of cracking, a similar crack pattern, and crack sizes compatible with each of the other panels. While speculative, it can be inferred that the service performance of bridge decks reinforced with each of the reinforcement types investigated would be very similar.

The mode of failure of each of the slab panels was consistent with diagonal tension shear. However, this is not to suggest the performance of any of the slab panels was other than that intended by the AASHTO Specifications. In fact, with an assumed 20% redistribution of moments, the full-scale slab panels consistently showed moment capacities in excess of those predicted by moment-curvature analysis, and well in excess of the AASHTO factored design moment. Experimental moment capacities exceeding those computed by moment-curvature analysis indicate that in each case the tensile strains mobilized in the reinforcement was more than adequate to develop the full bending capacity of the concrete section prior to diagonal tension shear failure.

Owing to the difficulties of measuring and evaluating in-service performance from quasi-static laboratory testing, field inspection of the two bridges in which the various reinforcements considered in this study were deployed is necessary and the most effective means by which to evaluate their respective behaviors. Field inspections of the CFRP reinforced bridge deck have been performed over the past 1½ years. Field inspections of the SSC and MMFX reinforced bridge deck started in October 2002.

REFERENCES

ACI Committee 318, *Building Code Requirements for Structural Concrete (ACI 318-02) and Commentary (ACI 318R-01)*, American Concrete Institute, Farmington Hills, MI 48333.

AASHTO, *Standard Specification for Highways Bridges*, 17th Edition, 444 North Capital Street, N.W., Suite 249, Washington, D.C., 2002.

American Society for Testing and Materials, *Annual Book of ASTM Standards, Vol. 04. 02 (Concrete and Mineral Aggregates)*, 1991.

Richard, R. M., and Blalock, J. R. (1969), "Finite Element Analysis of Inelastic Structures", *AIAA J.* 7(3), 432-8.

Hognestad, E., "A study of Combined Bending and Axial Load in Reinforced Concrete Members," Bulletin Series No. 399, University of Illinois Engineering Experiment Station, 1951, 46p.